Insect Biochemistry and Molecular Biology 40 (2010) 742–751

Contents lists available at ScienceDirect

Insect Biochemistry and Molecular Biology

journal homepage: www.elsevier.com/locate/ibmb

Neofunctionalization in an ancestral insect desaturase lineage led to rare Δ^6 pheromone signals in the Chinese tussah silkworm

Hong-Lei Wang [a,b,1], Marjorie A. Liénard [a,1], Cheng-Hua Zhao [b], Chen-Zhu Wang [b], Christer Löfstedt [a,*]

[a] Chemical Ecology and Ecotoxicology, Department of Biology, Lund University, SE-223 62 Lund, Sweden
[b] State Key Laboratory of Integrated Management of Pest Insects and Rodents, Institute of Zoology, Chinese Academy of Sciences, Beijing 100101, China

ARTICLE INFO

Article history:
Received 27 May 2010
Received in revised form
2 July 2010
Accepted 26 July 2010

Keywords:
Lepidoptera
Antheraea pernyi
Pheromone biosynthesis
Gene family evolution
Mating communication
Δ^6 desaturase
Δ^{11} desaturase

ABSTRACT

The Chinese tussah silkworm, *Antheraea pernyi* (Lepidoptera: Saturniidae) produces a rare dienoic sex pheromone composed of (*E,Z*)-6,11-hexadecadienal, (*E,Z*)-6,11-hexadecadienyl acetate and (*E,Z*)-4,9-tetradecadienyl acetate, and for which the biosynthetic routes are yet unresolved. By means of gland composition analyses and *in vivo* labeling we evidenced that pheromone biosynthesis towards the immediate dienoic gland precursor, the (*E,Z*)-6,11-hexadecadienoic acid, involves desaturation steps with Δ^6 and Δ^{11} regioselectivity. cDNA cloning of pheromone gland desaturases and heterologous expression in yeast demonstrated that the 6,11-dienoic pheromone is generated from two biosynthetic routes implicating a Δ^6 and Δ^{11} desaturase duo *albeit* with an inverted reaction order. The two desaturases first catalyze the formation of the (*E*)-6-hexadecenoic acid or (*Z*)-11-hexadecenoic acid, key mono-unsaturated biosynthetic intermediates. Subsequently, each enzyme is able to produce the (*E,Z*)-6,11-hexadecadienoic acid by accommodating its non-respective mono-unsaturated product. Besides elucidating an unusually flexible pheromone biosynthetic pathway, our data provide the first identification of a biosynthetic Δ^6 desaturase involved in insect mate communication. The occurrence of this novel Δ^6 desaturase function is consistent with an evolutionary scenario involving neo-functionalization of an ancestral desaturase belonging to a gene lineage different from the Δ^{11} desaturases commonly involved in moth pheromone biosynthesis.

1. Introduction

Many animals have evolved finely tuned intraspecific communication systems including visual, acoustic or chemical cues in order to achieve reproduction. In most moths, females release mixtures of long-chain C_{10} to C_{18} fatty acyl derivatives that serve as chemical signals to accurately attract conspecific males (Roelofs, 1995). Subtle variations in structure (carbon chain length and double bond location) and composition of the pheromone blends (number of components and their ratio) differentiate the signals from closely related species (Ando et al., 2004) and can enhance pre-zygotic reproductive isolation. *In vivo* studies using deuterium-labeled precursors showed that pheromone molecules are in most cases derived by discrete sequential modifications of ubiquitous fatty acid precursors such as palmitic or stearic acids through combinations of limited chain shortening and desaturation followed by modification of the carbonyl end into an alcohol, aldehyde or acetate (Bjostad et al., 1987; Blomquist et al., 2005).

The observed structural variation found among extant moth sex pheromones is consistent with the evolution of a few key enzymes acting in concert in the female pheromone gland, including a large repertoire of sex pheromone biosynthetic desaturases exhibiting unique enzymatic activities (reviewed in Blomquist et al., 2005). Members of the lepidopteran desaturase gene family are membrane-bound enzymes homologous to the metabolic non-heme diiron acyl-CoA Z9-desaturases introducing a Δ^9 double bond in palmitoyl-CoA (C_{16}) and stearoyl-CoA (C_{18}) across plant and animal taxa, and are phylogenetically unrelated to soluble plant desaturases (Shanklin and Cahoon, 1998). Desaturase genes involved in moth pheromone production encode several functional classes introducing double bonds at specific locations along the carbon chain in saturated and unsaturated acyl chains (Roelofs and Rooney, 2003), displaying *cis* and/or *trans* stereo-selectivity and distinct regio-specificity (*e.g.* Δ^9, Δ^{10}, Δ^{11}, Δ^{14} or bifunctional $\Delta^{11/10,12}$ or $\Delta^{11/11,13}$) (*e.g.* Knipple et al., 1998; Roelofs et al., 2002; Serra et al., 2006, 2007). In females of the Chinese tussah silkworm *Antheraea pernyi*, the pheromone gland located between the 8th and 9th

* Corresponding author. Tel.: +46 46 222 9338; fax: +46 46 222 4716.
E-mail address: christer.lofstedt@ekol.lu.se (C. Löfstedt).
[1] These authors contributed equally to this work.

0965-1748/$ – see front matter © 2010 Elsevier Ltd. All rights reserved.
doi:10.1016/j.ibmb.2010.07.009

terminal abdominal segments (Percy-Cunningham and MacDonald, 1987) produces a dienoic sex pheromone system composed of (*E,Z*)-6,11-hexadecadienal (*E*6,*Z*11-16:Ald), (*E,Z*)-6,11-hexadecadienyl acetate (*E*6,*Z*11-16:OAc) and its chain shortened form, the (*E,Z*)-4,9-tetradecadienyl acetate (*E*4,*Z*9-14:OAc) (Bestmann et al., 1987). The biosynthesis towards these dienoic components presumably requires two desaturation steps and the location of one of the double bonds in 11th position, which is common among moth species, suggests the involvement of a Δ^{11} desaturase (*e.g.*,Tillman et al., 1999; Blomquist et al., 2005). On the other hand, double bonds located at the 6th carbon position in the fatty acyl chain are very rare. Besides their existence in species of the *Antheraea* genus (Bombycoidea: Saturniidae) (Bestmann et al., 1987; Kochansky et al., 1975), they have only been reported in a few moth species of the *Stathmopoda* genus (Gelechioidea: Oecophoridae) (Naka et al., 2003) and no Δ^6 desaturases have been identified in insects so far.

In this study, we elucidated the biosynthetic pathway towards the sex pheromone of *A. pernyi* by means of gland precursor analyses and *in vivo* labeling. We then functionally characterized the candidate desaturase cDNAs from *A. pernyi* pheromone glands and determined their specific functionalities *in vitro*. Heterologous expression revealed that two genes, which encode desaturases exhibiting Δ^{11} and Δ^6 biochemical activities account for the production of the (*E,Z*)-6,11-hexadecadienoic acid, the major sex-pheromone precursor in this species. Our results reveal an unusual flexibility in the order of the desaturation steps taking place during sex pheromone biosynthesis and provide the first example of a Δ^6 desaturase involved in mate communication in Lepidoptera.

2. Materials and methods

2.1. Insect collection and sex pheromone gland extracts

Cocoons of *A. pernyi* were obtained from the Sericultural Research Institute of Liaoning Province (Fengcheng, China). The pupae were gently removed from the silk cocoons, sexed and maintained at 23 ± 1 °C under a 16 h:8 h light:dark cycle. Sex pheromone glands (PGs) of 1- to 2-day-old virgin females were dissected at 5–7 h into the scotophase and individual PGs were extracted for 15 min at room temperature in 30 μl hexane contained in a 300-μl insert placed in a 2-ml screw-cap vial (Agilent). The hexane extract was transferred to a clean insert and the gland lipid content was subsequently extracted with 50 μl chloroform/methanol (2:1, v:v) for 24 h at 4 °C. The gland was removed and the extract was concentrated to dryness under a gentle stream of nitrogen. The residue was subjected to base methanolysis to convert fatty acyl moieties to the corresponding methyl esters (Roelofs and Bjostad, 1984). The resulting hexane extracts and gland fatty acid methyl esters (FAMEs) were analyzed by GC-MS or GC-FID as described in section 2.3. The double bond positions of mono- and di-unsaturated methyl esters were determined by DMDS derivatization (Buser et al., 1983; Dunkelblum and Silk, 1985; Attygalle, 1998) prior to GC-MS analyses.

2.2. In vivo labeling

Three deuterium-labeled fatty acids, potential pheromone precursors, were used to probe the pheromone biosynthetic pathway. The (14,14,14-D_3)-tetradecanoic acid (D_3-14:Acid) and (16,16,16-D_3)-hexadecanoic acid (D_3-16:Acid) were purchased from Larodan Fine Chemicals (Malmö, Sweden). The (*Z*)-[13,13,14,14,15,15,16,16,16-D_9]-11-hexadecenoic acid (D_9-*Z*11-16:Acid) was from our laboratory collection of pheromone precursors and its synthesis was described in Löfstedt et al. (1994). Each labeled fatty acid was dissolved in dimethylsulfoxide (DMSO) at a concentration of 40 μg/μl. Using a 10-μl-Hamilton syringe, 0.2 μl were topically applied at 4–5 h into the scotophase to an extruded female PG and incubated for one hour. Each experiment was performed in parallel with DMSO-only as controls. Pheromone and precursor extracts were prepared as described in section 2.1, prior to GC-MS analyses.

2.3. Gas chromatography and mass spectrometry analyses

Pheromone gland extracts and fatty acyl moieties were analyzed by gas chromatography on a Hewlett–Packard HP 5890II GC equipped with a flame ionization detector and a BP-20 capillary column (50 m × 0.25 mm i.d., SGE). The oven temperature was programmed at 80 °C for 1 min, then increased to 210 °C at a rate of 10 °C/min and held for 20 min. Compounds were identified by comparing their retention times with authentic references (see additional Material and Methods) and their mass spectra obtained from an Agilent 6890N GC system coupled with an Agilent 5973N mass selective detector and a BPX-70 capillary column (50 m × 0.25 mm × 0.25 μm, SGE). The incorporation of deuterium labels into pheromone compounds, including saturated and unsaturated analogs, and fatty acyl moieties was determined by GC-MS under the selective ion monitoring (SIM) mode The oven temperature program used in GC-MS analysis was identical to that used in GC-FID analysis. Yeast FAME samples were analyzed on a Hewlett Packard HP 5890II GC system coupled with an HP 5972 mass selective detector and an HP-INNOWax capillary column (30 m × 0.25 mm × 0.25 μm, Agilent). The oven temperature was programmed at 80 °C for 1 min, raised to 210 °C at a rate of 4 °C/min and held for 10 min, then raised to 230 °C at a rate of 10 °C/min and held for 20 min. DMDS derivatives were analyzed on an Agilent 6890 GC system coupled with an HP 5973 mass selective detector and an HP-5MS capillary column (30 m × 0.25 mm × 0.25 μm, Agilent). The oven temperature was set at 80 °C for 1 min, raised to 140 °C at a rate of 20 °C/min, then to 250 °C at a rate of 4 °C/min and held for 20 min.

2.4. cDNA cloning of desaturases

First strand cDNA was synthesized from total RNA isolated from *A. pernyi* PGs prior to PCR amplification using primers designed on desaturase conserved histidine-rich motifs, forward: 5′-GGYATY ACVGCHGGNGCWCA-3′, reverse: 5′-TGRTARTTRTGGAABSCYTCNCC-3′ (Roelofs et al., 2002) that targeted a DNA fragment encompassing the central region of a desaturase gene. The thermal cycling conditions consisted in 95 °C for 5 min, 35 cycles at 95 °C for 30 s, 50 °C for 45 s, 72 °C for 90 s, and 72 °C for 10 min. After agarose gel electrophoresis, the expected 560-bp DNA fragment was excised and purified using the QIAquick gel extraction kit (Invitrogen), cloned into the TOPO TA pCR2.1 vector (Invitrogen) and transformed into TOPO 10 cells (Invitrogen). Plasmid DNAs were purified and positive clones were subjected to sequencing using the Big Dye Terminator (Applied Biosystems) followed by sequence analysis on a capillary ABI 3100 sequencer instrument (Applied Biosystems). Sequence analysis indicated the presence of three distinct cDNAs related to other moth desaturases, including the ubiquitous Δ^9 desaturase. The 3′- and 5′-cDNA termini were obtained using the SMART RACE technology (Clontech) and gene-specific primers (GSPs) (Table 1). GSPs designed at the 5′ and 3′ends (Table 2) were subsequently used to amplify the entire gene regions and verify each gene's full-length sequence integrity.

2.5. Functional assay

The *Ape*-PGΔ11 or *Ape*-PGΔx ORFs were amplified using the Advantage2 PCR system (Clontech) and GSPs encompassing the

Table 1
Primer sets used for amplifying 5′and 3′ desaturase cDNA termini.

Primer name	Primer sequence
Ape-QPTQ-5RACE	5′-CCCAAGTGATCGCGGTGTTTTGAA-3′
Ape-QPTQ-5RACE_nested	5′-GATCAGCATCGGTATCAGTGAACTT-3′
Ape-QPTQ-3RACE	5′-CAATGCATGGCATGCAACAGTTTTCA-3′
Ape-QPTQ-3RACE_nested	5′-TAGTGCCGCACATATGTGGGGTTA-3′
Ape-KPAE-5RACE	5′-CGTTGCTTTGAAACATCTGTGGCTC-3′
Ape-KPAE-5RACE_nested	5′-GGTGAGAGCGAACATCAGGAACAAT-3′
Ape-KPAE-3RACE	5′-TGGTGAATCTAATGGCTGCGTTCG-3′
Ape-KPAE-3RACE_nested	5′-GCTTGGCAATGCTTCGTTCGGTAC-3′

BamH1 and *EcoR1* restriction sites (Table 2). The PCR products were purified, digested and subcloned into the linearized pYEX-CHT vector (Patel et al., 2003). Recombinant plasmids were propagated in TOPO 10 cells, purified and verified by sequencing. The empty pYEX-CHT or the pYEX-CHT-*Ape*-PGΔx and pYEX-CHT-*Ape*-PGΔ11 constructs were transformed into the *elo1 ole1* strain of the yeast *Saccharomyces cerevisiae* (*MATa elo1::HIS3 ole1::LEU2 ade2 his3 leu2 ura3*) (Schneiter et al., 2000) and grown for 4 days at 30 °C on selective plates containing 0.69% YNB and a complete drop-out lacking Uracil and Leucine (ForMedium), 2% Glucose, 0.01% Adenine, 1% Tergitol (NP-40, Sigma) and 0.5 mM unsaturated fatty acids (palmitoleic and/or oleic acids) (Sigma). Individual prototroph colonies were inoculated in 5 ml selective medium for 48 h at 30 °C and 300 rpm shaking, diluted to an $OD_{600} = 0.4$ in 250 ml-flasks containing 20 ml Sc-Ura-Leu medium and 2 mM $CuSO_4$ without or with addition of the pheromone biosynthetic intermediates (*i.e.* 0.5 mM of *Z*11-16:Me or *E*6-16:Me) and grown for 48 h at 30 °C and 200 rpm shaking. After induction, yeast cells were collected by centrifugation and washed with sterile water. Total lipids were extracted with chloroform/methanol (2:1 v:v) followed by base-methanolysis, and methyl esters were recovered in hexane prior to GC-MS analyses. The position of double bonds in monoenes and dienes was determined by DMDS derivatization followed by GC-MS analyses.

3. Results

3.1. Pheromone gland composition and analysis of pheromone biosynthetic precursors

In addition to the three sex pheromone components previously identified, *i.e.* the *E*6,*Z*11-16:Ald, *E*6,*Z*11-16:OAc and *E*4,*Z*9-14:OAc (Bestmann et al., 1987), GC-MS analyses revealed other gland constituents, *i.e.* saturated and monounsaturated C_{16} aldehydes and acetates such as hexadecanal (16:Ald), (*E*)-6-hexadecenal (*E*6-16:Ald), (*Z*)-11-hexadecenal (*Z*11-16:Ald), hexadecanyl acetate (16:OAc), (*E*)-6-hexadecenyl acetate (*E*6-16:OAc) and (*Z*)-11-hexadecenyl acetate (*Z*11-16:OAc) (Fig. 1A). GC-MS analyses of gland lipids in the form of fatty acid methyl esters (FAMEs) indicated that besides ubiquitous fatty acids, several unusual acyl moieties were present in the female gland, namely the mono-unsaturated (*E*)-4- and (*Z*)-9-tetradecenoate (*E*4- and *Z*9-14:Me), (*E*)-6-, (*Z*)-6- and (*Z*)-11-hexadecenoate (*E*6-, *Z*6- and *Z*11-16:Me), (*Z*)-11- and (*Z*)-13-octadecenoate (*Z*11- and *Z*13-18:Me), as well as the diunsaturated (*E*,*Z*)-4,9-tetradecadienoate (*E*4,*Z*9-14:Me) and the (*E*,*Z*)-6,11-hexadecadienoate (*E*6,*Z*11-16:Me) (Table 3). The double bond position and geometry in mono- and diunsaturated methyl esters were confirmed by dimethyl disulfide (DMDS) derivatization followed by GC-MS analyses, and by comparing their mass spectra and retention times with those of synthetic standards.

3.2. Biosynthetic routes towards A. pernyi sex pheromone

D_3-14:Acid, D_3-16:Acid and D_9-*Z*11-16:Acid were dissolved in DMSO and topically applied to the sex pheromone gland of adult females along with DMSO-only controls. GC-MS analyses of PG extracts showed that topical application of the D_3-14:Acid did not lead to any deuterium incorporation into either pheromone gland components or fatty acid moieties (data not shown). In contrast, topical applications of D_3-16:Acid showed that three deuterium atoms were incorporated into the *E*6- and *Z*11-16:Ald/OAc as indicated by ions at *m*/*z* 223 and 225, the *E*6,*Z*11-16:Ald/OAc as indicated by ions at *m*/*z* 221 and 283, respectively, as well as the chain-shortened *E*4,*Z*9-14:OAc, as indicated by the ion at *m*/*z* 195 (Fig. 1B). Three deuterium atoms from D_3-16:Acid were also incorporated in the 14:Me, the *E*6- and *Z*11-16:Me and the *E*6,*Z*11-16:Me, as indicated by ions at *m*/*z* 245, 239 and 269, respectively (Fig. 1C).

When topically applying the D_9-*Z*11-16:Acid, nine deuterium atoms were incorporated into the *Z*11-16:Ald/OAc as indicated by ions at *m*/*z* 229 and 231, respectively, the diunsaturated *E*6,*Z*11-16:Ald/OAc as well as the chain-shortened *E*4,*Z*9-14:OAc, as indicated by ions at *m*/*z* 227, 289 and 201, respectively (Fig. 1D). Also, nine deuterium atoms from the D_9-*Z*11-16:Acid were incorporated into two direct precursors, the *E*6,*Z*11-16:Me and the *E*4,*Z*9-14:Me as indicated by ions at *m*/*z* 275 and 247, respectively (Fig. 1E). The label was also found incorporated into the chain-shortened *Z*9-14:Me (Fig. 1E) and into the chain-elongated *Z*13-18:Me (Fig. S1) as indicated by ions at *m*/*z* 217 and 273, respectively.

3.3. Cloning of fatty-acyl desaturases

Three distinct desaturase cDNAs were cloned by using *A. pernyi* PG cDNA in PCR reactions with degenerated oligonucleotide primers (Roelofs et al., 2002) targeting the characteristic histidine-rich domains of fatty acid desaturases (Shanklin and Cahoon, 1998;

Table 2
Primer sets used for full-length gene verification and desaturase expression.

Primer name	Primer sequence[a]	Amplicon size (bp)
Ape-QPTQ-fl-s	5′-GAGTCTGTTGATTTTCATGAACAACG-3′	
Ape-QPTQ-fl-as1	5′-AGGGAATCTGAATATATGATTATAATAAAGT-3′	1160
Ape-QPTQ-fl-as2	5′-TCATTACTTGGCTACATCACACAATTAA-3′	1405
Ape-KPAE-fl-s	5′-AAGCAGTGGTATCAACGCAGAGTACG-3′	
Ape-KPAE-fl-as	5′-TTACATCCATATAAGGGCCTCCAA-3′	1821
Ape-QPTQ-ORFs-BamH1	5′-ggatccGTTATGGCTCCGTATACTGAAA-3′	
Ape-QPTQ-ORFas-EcoR1	5′-gaattcGATTAAAAAGCACTTTTATGAACGTAG-3′	1046
Ape-KPAE-ORFs-BamH1	5′-ggatccATCATGGAAATAATAAAATTTGACG-3′	
Ape-KPAE-ORFas-EcoR1	5′-gaattcCACTAAGATTTTAATAAATCATCAC-3′	963

[a] Restriction sites are indicated in lower case letters, START and STOP codons are underlined.

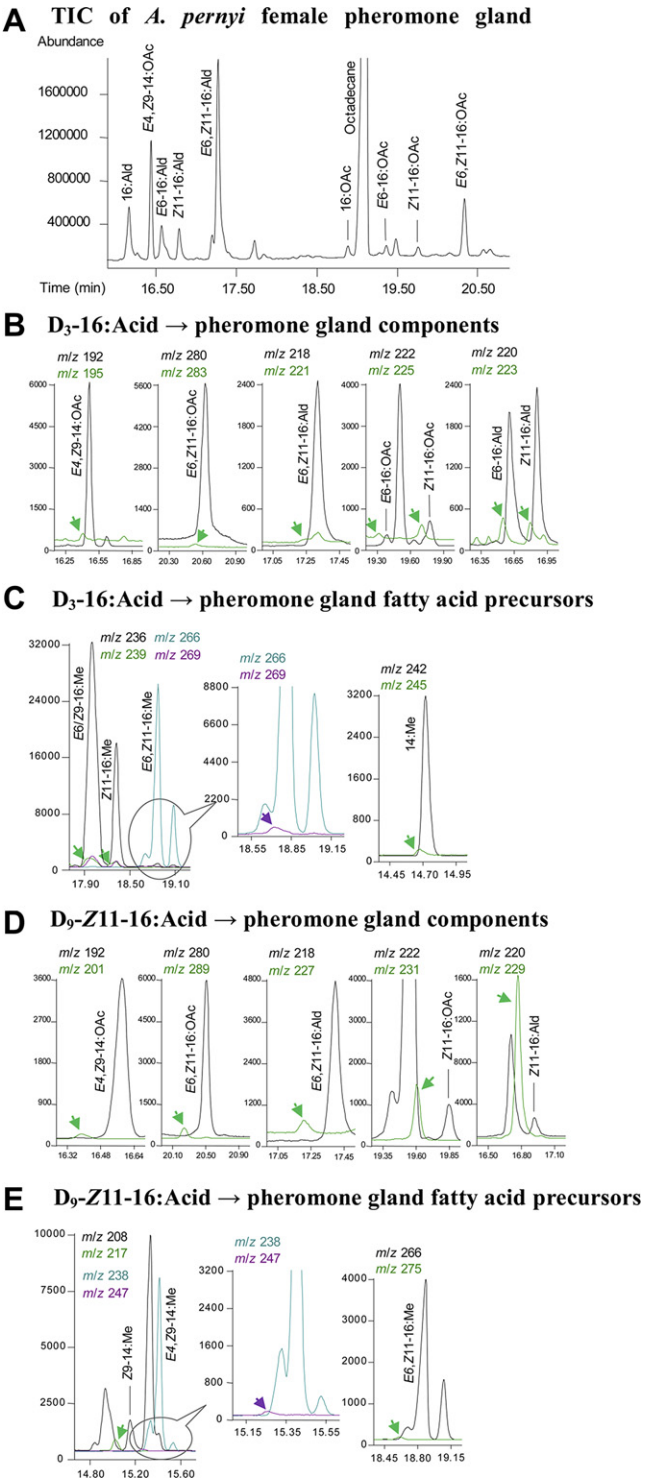

Fig. 1. Total ion chromatogram (TIC) of an *Antheraea pernyi* female pheromone gland extract analyzed by GC-MS in scan mode (A). (B-E) Selective ion monitoring (SIM) of label incorporation from D_3-16:Acid or D_9-*Z*11-16:Acid into pheromone gland components (B and D, respectively) and fatty acyl precursors (C and E, respectively). *Y*-axes represent the relative abundance and *x*-axes indicate the retention times (min). Green or purple arrows indicate the incorporation of deuterium labels. The native, D_3- or D_9-labeled pheromone gland components were monitored by their diagnostic ions and diagnostic ions +3 or +9, respectively: *E*6-16:Ald and *Z*11-16:Ald: *m/z* 220, 223, 229; *E*6-16:OAc and *Z*11-16:OAc: *m/z* 222, 225, 231; *E*6,*Z*11-16:Ald: *m/z* 218, 221, 227; *E*6,*Z*11-16:OAc: *m/z* 280, 283, 289; *E*4,*Z*9-14:OAc: *m/z* 192, 195, 201. The native, D_3- or D_9-labeled fatty acid methyl ester precursors were monitored by their diagnostic ions and diagnostic ions +3 or +9: *E*6-16:Me and *Z*11-16:Me: *m/z* 236, 239; *E*6,*Z*11-16:Me: *m/z* 266, 269, 275; *E*4,*Z*9-14:Me: *m/z* 238, 247; *Z*9-14:Me: *m/z* 208, 217; 14:Me: *m/z* 242, 245.

Table 3
Fatty acid methyl esters identified from the sex pheromone gland of *Antheraea pernyi* females.[a]

Component	Amount (ng/female)[b]	Ratio
14:Me	418 ± 88	4.3 ± 1.3
*Z*4-14:Me[c]	Trace	/
*E*4-14:Me	311 ± 86	3.3 ± 1.3
*Z*5-14:Me[c]	Trace	/
*Z*9-14:Me	279 ± 87	3.0 ± 1.4
*Z*11-14:Me[c]	Trace	/
*E*4,*Z*9-14:Me	612 ± 205	6.2 ± 1.9
16:Me	3866 ± 946	38.6 ± 6.5
*Z*6-16:Me	840 ± 318	8.3 ± 2.3
*E*6-16:Me	1293 ± 794	12.7 ± 6.8
*Z*7-16:Me[c]	Trace	/
*Z*9-16:Me	852 ± 202	8.6 ± 2.1
*Z*11-16:Me	1151 ± 370	11.8 ± 4.6
*E*6,*Z*11-16:Me	2722 ± 1346	26.8 ± 10.9
18:Me	4286 ± 976	43.2 ± 8.3
*Z*9-18:Me	10087 ± 2303	100
*Z*11-18:Me	5951 ± 2169	58.2 ± 14.0
*Z*13-18:Me	472 ± 117	4.8 ± 1.2
*Z*9,*Z*12-18:Me[d]	4831 ± 1708	47.7 ± 8.1
*Z*9,*Z*12,*Z*15-18:Me[d]	9344 ± 4308	90.0 ± 14.3

[a] Sex pheromone components were converted to their corresponding methyl esters (FAME) prior to GC-MS analyses. 1/240 female equivalent was analyzed using both GC-FID and GC-MS.
[b] All amounts (means ± SE, Nextracts = 10) were calculated using the linear regression equation $y = 1877.1x - 2338.6$ ($r^2 = 0.9939$), which was obtained based on the FID abundance of the external standard, Z9-16:Me.
[c] Component identification made based on DMDS derivatization.
[d] $N = 4$.

Shanklin et al., 1994). The sequences are deposited in the GenBank database with accession nos. GU952763–GU952765.

Sequence analysis revealed one transcript, named *Ape*-Δ9 to be highly homologous to sequences encoding Δ^9 desaturases from other moths. Its deduced protein shared more than 90% identity with Δ^9 desaturases that typically catalyze the formation of palmitoleic acid and oleic acid ($C_{16} > C_{18}$), as shown in *Ostrinia nubilalis* and *Choristoneura parallela* (GenBank accession nos. AF243047 and AAN39700) (Roelofs et al., 2002; Liu et al., 2004). Full-length sequences were obtained for the second and third pheromone gland desaturase transcripts only, because *in vivo* labeling did not predict pheromone biosynthesis to proceed through Δ^9-desaturation, similarly to many other moths where the ubiquitous Δ^9 desaturase is not required for pheromone biosynthesis (Roelofs and Rooney, 2003).

The full-length cDNAs for the second transcript spanned either 1161 or 1438 bp. These sequences differed only in the 3′UTR portion of the gene and encompassed an identical ORF of 1041 bp corresponding to a protein with 347 aa residues. The third full-length nucleotide sequence spanned 1862 bp and encompassed an ORF of 948 bp (316 aa residues). Both predicted proteins had all key features of fatty acyl desaturases including transmembrane spanning regions separating the three conserved his-rich catalytic domains (Shanklin et al., 1994; Hashimoto et al., 2008). Blast analyses revealed high aa sequence homology (>60%) between the second transcript, *Ape*-PGΔ11 and known Δ^{11} desaturases from related lepidopteran species, *i.e.* 67% identity with the pheromone biosynthetic $\Delta^{11/10,12}$ desaturase from *Manduca sexta* (GenBank accession no. CAJ27976).

The third desaturase cDNA, which we preliminary named *Ape*-PGΔx, had relatively little sequence identity with *Ape*-Δ9 (34%) and *Ape*-PGΔ11 (37%) and overall less than 40% aa sequence identity with all major Δ^9, Δ^{14} and Δ^{11} classes of moth pheromone desaturases identified so far. The best identity match at the amino acid sequence level was found to be 54 or 56% with partial sequences encompassing the central region of desaturases of yet unknown function (GenBank accession nos. AF482899 and AF482918) from

the moths *Cydia pomonella* and *Pectinophora gossypiella*, respectively. A phylogenetic reconstruction showed that the *Ape*-PGΔ11 clusters with the Lepidoptera-specific Δ^{11} desaturase subfamily (Fig. 2), whereas *Ape*-PGΔx clusters in a gene lineage different from either of the Δ^{9}, Δ^{14} or Δ^{11} pheromone desaturases (Fig. 2).

3.4. Functional assay of biosynthetic desaturases

In order to investigate their desaturase activity and substrate specificity, the *Ape*-PGΔ11 and *Ape*-PGΔx ORFs were cloned in the pYEX-CHT vector and expressed under the control of the

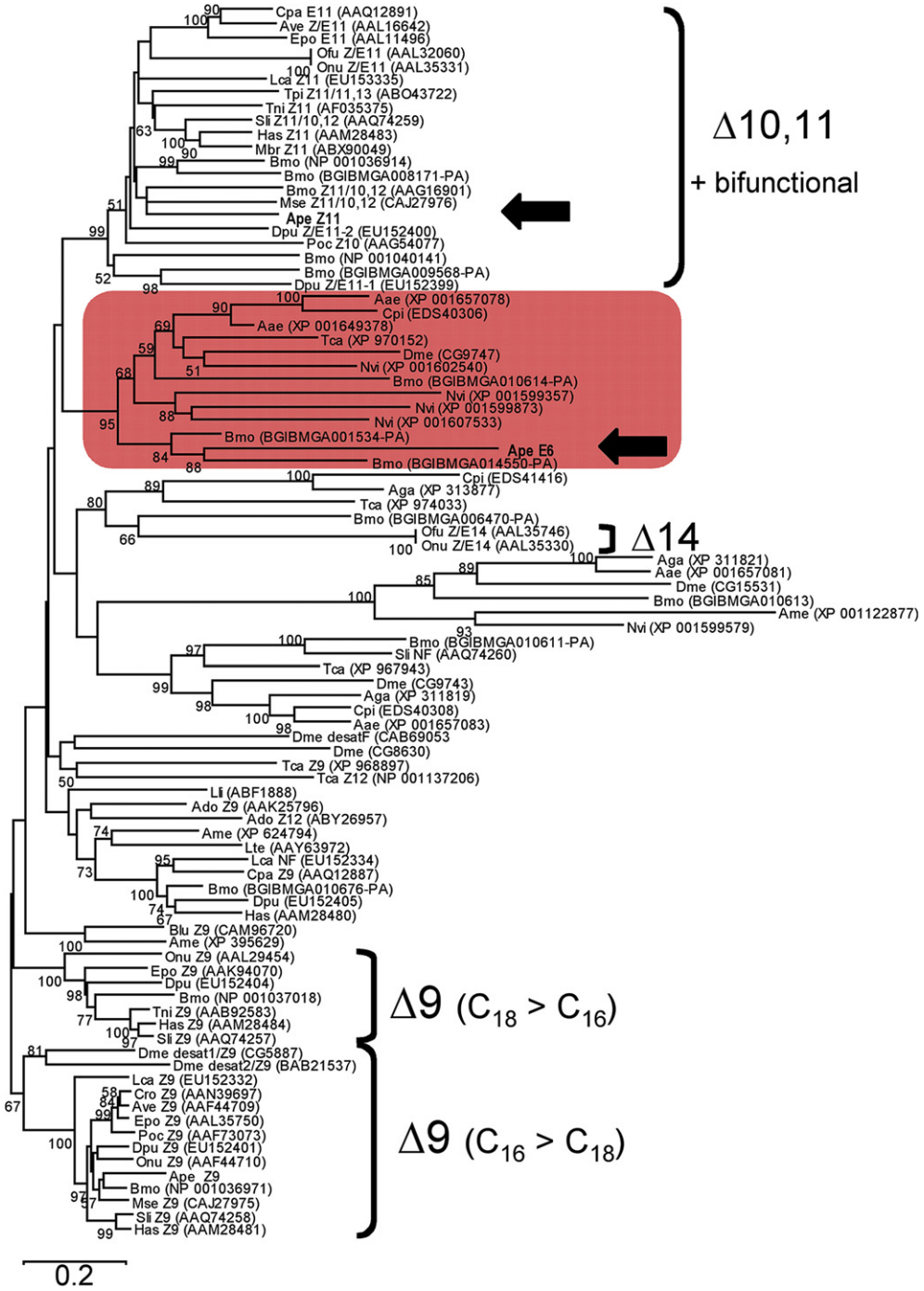

Fig. 2. Phylogeny of insect desaturases including the *Antheraea pernyi* Z11 and E6 desaturases. The clade highlighted in red represents the gene lineage comprising the novel Δ^{6} desaturase (shown with a black arrow). Selected full-length deduced protein sequences were retrieved from the GenBank non-redundant protein database or the silkworm database and aligned in MAFFTv6 (Katoh and Toh, 2008). The Neighbor-joining analysis was computed using the Molecular Evolutionary Genetics Analysis (MEGA version 4.0.), the JTT model for amino acids with pairwise comparisons and 1500 bootstrap replicates (Tamura et al., 2007). Sequences are named according to the abbreviated species, the desaturase biochemical activity when assayed (NF = non-functional); the protein accession numbers are in parentheses. The tree is rooted on the ancestral Δ^{9} desaturase $C_{16} > C_{18}$ lineage. The abbreviated names correspond to Coleoptera: Tca, *Tribolium castaneum*; Diptera: Aae, *Aedes aegypti*; Aga, *Anopheles gambiae*; Cpi, *Culex pipiens*; Dme, *Drosophila melanogaster*; Hemiptera: Lli, *Lygus lineolaris*; Lte, *Lysiphiebus testaceipes*; Hymenoptera: Ame, *Apis mellifera*; Blu, *Bombus lucorum*; Nvi, *Nasonia vitripennis*; Lepidoptera: Ape, *Antheraea pernyi*; Ave, *Argyrotaenia velutinana*; Bmo, *Bombyx mori*; Cro, *Choristoneura rosaceana*; Dpu, *Dendrolimus punctatus*; Epo, *Epiphyas postvittana*; Has, *Helicoverpa assulta*; Lca, *Lampronia capitella*; Mbr, *Mamestra brassicae*; Mse, *Manduca sexta*; Ofu, *Ostrinia furnacalis*; Onu, *O. nubilalis*; Poc, *Planotortrix octo*; Sli, *Spodoptera littoralis*; Tpi, *Thaumetopoea pityocampa*; Tni, *Trichoplusia ni*; Orthoptera: Ado, *Acheta domesticus* (For interpretation of the references to color in this figure legend, the reader is referred to the web version of this article.).

copper-inducible CUP1 promoter in the *ole1 elo1* strain of the yeast *Saccharomyces cerevisiae*. Lipid extracts of copper-induced yeast cells were base-methanolyzed and analyzed by GC-MS. FAME extracts from yeast transformed with the empty pYEX-CHT vector were also prepared to serve as control. In the latter case, GC-MS analyses showed the presence of saturated FAMEs common to yeast cell membranes in addition to the supplemented *Z*9-18:Me (Fig. 3A). Methanolyzed cells from Cu^{2+}-induced yeast transformed with the pYEX-CHT-*Ape*-PGΔ11-ORF contained high amounts of *Z*11-16:Me and *Z*11-18:Me in addition to minor amounts of $\Delta^{11\text{-}12}$:Me and *Z/E*11-14:Me (Fig. 3B). The corresponding DMDS adducts exhibited a common ion at *m/z* 245, characteristic of a double bond in position Δ^{11} in the acyl chain (Fig. 4B). Cu^{2+}-induced yeast transformed with the pYEX-CHT-*Ape*-PGΔx-ORF contained *Z*6- and *E*6-16:Me (Fig. 3C). The double bond position from the natural compounds was confirmed by comparing both retention times and mass spectra of their DMDS adducts with authentic synthetic references. They exhibited the molecular ion characteristic of monounsaturated C_{16} methyl esters at *m/z* 362 in addition to characteristic ions of methyl Δ6-hexadecenoates at *m/z* 175 and 187 (Fig. 4A). This desaturase was accordingly renamed *Ape*-PGΔ6. Interestingly, the latter enzyme also produced minor amounts of *Z*11-16:Me (Figs. 3C and 4A). When supplemented with *E*6-16:Me, the pYEX-CHT-*Ape*-PGΔ11 catalyzed the formation of *E*6,*Z*11-16:Me (Fig. 3D). Similarly, when supplemented with *Z*11-16:Me, the pYEX-CHT-*Ape*-PGΔ6 produced the *E*6,*Z*11-16:Me, with no detectable trace of the (*Z*,*Z*) isomer (Fig. 3E). DMDS derivatization confirmed the presence of *E*6,*Z*11-16:Me adducts in both cases, which exhibited the same retention time as an authentic reference and a mass spectrum including the characteristic fragments at *m/z* 392 (M^+), 169 (base peak), 275, 217 and 227 (Fig. 4).

All together, the two *A. pernyi* PG desaturases encode functional enzymes that exhibited Δ^6 and Δ^{11} desaturase activities consistent with a role in the biosynthesis of the mono-unsaturated *E*6-16:Me or *Z*11-16:Me. Each enzyme was also capable of producing the *E*6,*Z*11-16:Me when supplemented with the appropriate monoenoic substrate. No mono- or di-unsaturated biosynthetic intermediates were produced in yeast cells carrying the empty pYEX-CHT plasmid, thereby supporting the conclusion that both the *Ape*-PGΔ6 and *Ape*-PGΔ11 are exhibiting desaturase activities consistent with a role in pheromone biosynthesis in this species.

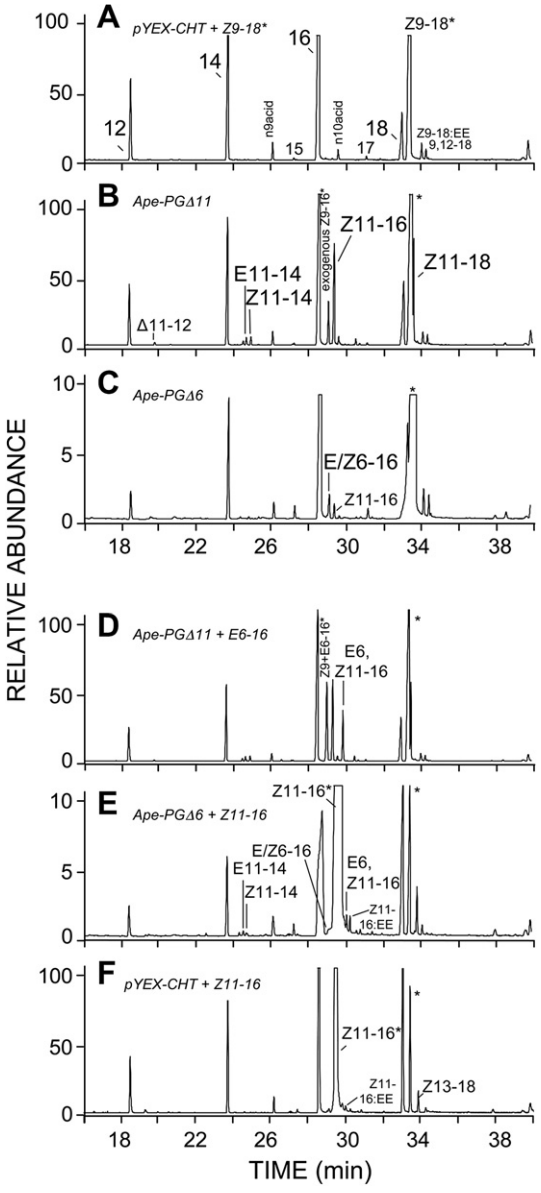

Fig. 3. GC-MS analyses of methanolyzed lipid extracts from Cu^{2+}-induced yeast transformed with desaturase genes from *A. pernyi*. The asterisks (*) indicate the supplemented unsaturated fatty acyls. The panels represent the total ion chromatograms (TICs) from (A) the empty pYEX-CHT, (B) pYEX-CHT-*Ape*-PGΔ11 (C) pYEX-CHT-*Ape*-PGΔ6, (D) pYEX-CHT-*Ape*-PGΔ11 supplemented with 0.5 mM *E*6-16:Me, (E-F) pYEX-CHT-*Ape*-PGΔ6 and pYEX-CHT alone supplemented with 0.5 mM *Z*11-16:Me. Since the *elo2* gene is active in the *ole1 elo1* strain of the yeast *S. cerevisiae*, the presence of *Z*13-18:Me in experiments E and F can be rationalized as elongation product of the supplemented *Z*11-16:Me and not from direct desaturation. All methyl esters were identified based on their mass spectra and comparison of their retention times with corresponding synthetic standards. The double bond positions were confirmed by DMDS derivatization (see Fig. 4). The abbreviations used correspond to: 12, methyl dodecanoate; Δ11-12, methyl Δ11-dodecenoate; 14, methyl tetradecanoate; *E*/*Z*11-14, methyl (*E*/*Z*)-11-tetradecenoate; n9acid, nonanoic acid; 15, methyl pentadecanoate; 16, methyl hexadecanoate; *E*/*Z*6-16, methyl (*E*/*Z*)-6-hexadecenoate; *Z*9-16, methyl (*Z*)-9-hexadecenoate, *Z*11-16, methyl (*Z*)-11-hexadecenoate; *E*6,*Z*11-16, methyl (*E*,*Z*)-6,11-hexadecadienoate; n10acid, decanoic acid; *Z*11-16:EE, ethyl (*Z*)-11-hexadecenoate; 17, methyl heptadecanoate; 18, methyl octadecanoate; *Z*9-18, methyl (*Z*)-9-octadecenoate; *Z*11-18, methyl (*Z*)-11-octadecenoate; *Z*9-18:EE, ethyl (*Z*)-9-octadecenoate; *Z*13-18, methyl (*Z*)-13-octadecenoate; 9,12-18, methyl (*Z*,*Z*)-9,12-octadecadienoate.

4. Discussion

The emergence of new types of desaturases in moth pheromone biosynthesis has been acknowledged as a key factor among the multifaceted evolutionary mechanisms towards the diversification among moth mating signals (Roelofs et al., 2002; Liénard et al., 2008). The discovery of a Δ^6 desaturase involved in the production of a rare *E*6,*Z*11-dienoic pheromone in the Chinese tussah silkworm provides evidence for neo-functionalization in an ancient insect desaturase lineage. The elucidation of *A. pernyi* pheromone biosynthesis by means of *in vivo* labeling, molecular characterization and *in vitro* heterologous expression of pheromone gland desaturase genes revealed that the new Δ^6 desaturase is capable of interacting with saturated but also *cis*-11-unsaturated fatty acyl precursors. In addition, the reversed combination of Δ^{11}- and Δ^6-desaturation reactions accredits a scenario with two alternative biosynthetic routes towards a single dienoic pheromone precursor in this moth species (Fig. 5).

4.1. A dual pheromone biosynthetic pathway involves two distinct desaturases with Δ^{11}- and Δ^6-regioselectivity

The composition of volatiles from the sex pheromone gland of *A. pernyi* involves three dienoic pheromone components, *i.e.* the *E*6,*Z*11-16:Ald, *E*6,*Z*11-16:OAc and *E*4,*Z*9-14:OAc (Bestmann et al., 1987) and minor amounts of the monounsaturated *E*6- and *Z*11-C_{16} aldehydes and acetates (Fig. 1A). This unique composition combined with corresponding *E*6-/*Z*11-C_{16} fatty acid intermediates

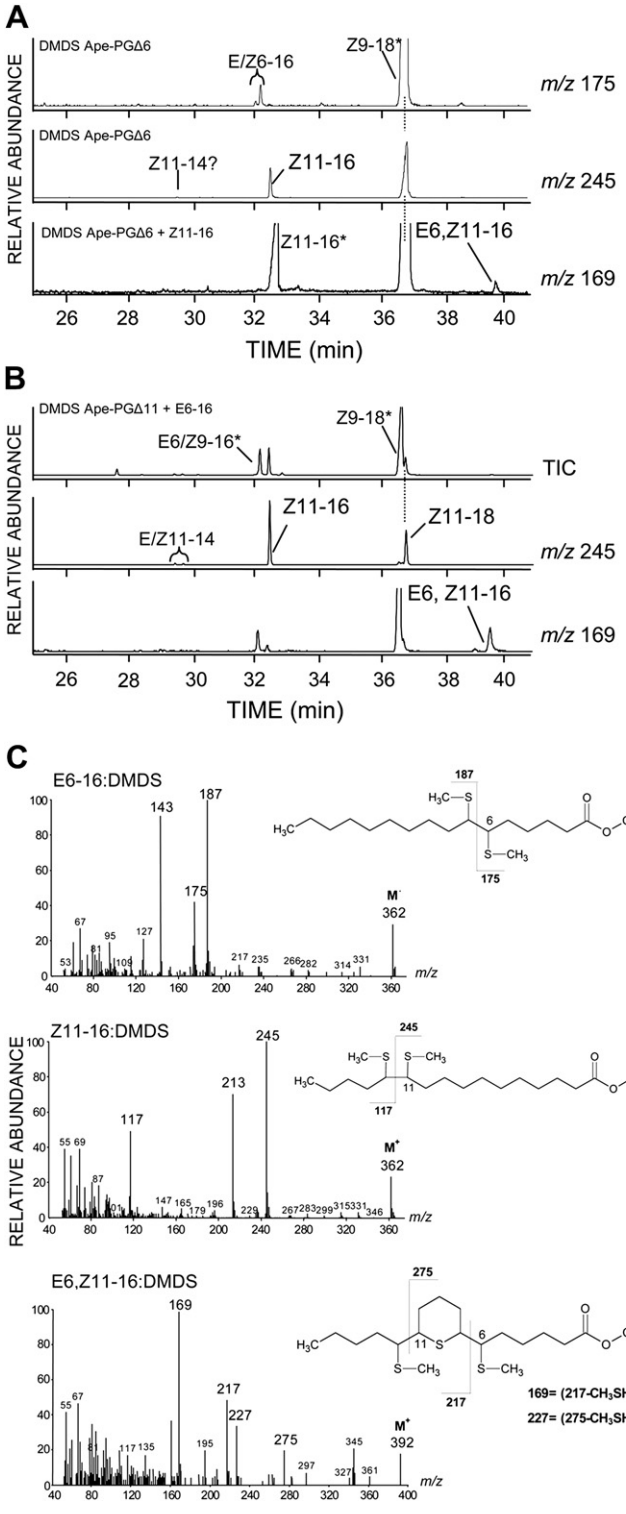

Fig. 4. Dimethyl disulfide (DMDS) adducts of FAME extracts from yeast transformed with (A) pYEX-CHT-*Ape*-PGΔ6 and (B) pYEX-CHT-*Ape*-PGΔ11. Asterisks (*) refer to DMDS adducts from supplemented unsaturated fatty acyls. (A) The chromatogram traces represent the TIC chromatograms obtained by selection of ions characteristic of a Δ^6 double bond (*m/z* at 175), of a Δ^{11} double bond (*m/z* at 245) and double bonds at $\Delta^{6,11}$ (*m/z* at 169). (B) TIC chromatogram from pYEX-CHT-*Ape*-PGΔ11 transformants grown in presence of the biosynthetic intermediate *E*6-16:Me and chromatogram traces obtained by selection of the characteristic ions at *m/z* 245 and 169, respectively. (C) Mass spectra of DMDS adducts of methyl (*E*)-6-hexadecenoate (*E*6-16:DMDS), of methyl (*Z*)-11-hexadecenoate (*Z*11-16:DMDS) and of methyl (*E,Z*)-6,11-hexadecadienoate (*E6,Z*11-16:DMDS).

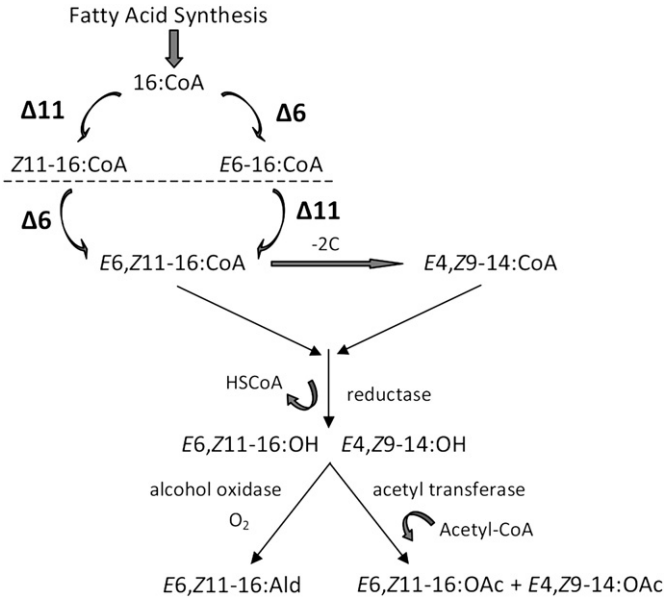

Fig. 5. Proposed dual biosynthetic pathway towards the Chinese tussah silkworm, *Antheraea pernyi* sex pheromone.

in the gland, and deuterium label incorporation from D_3-16:Acid into Δ^6- and Δ^{11}-unsaturated pheromone components and gland precursors as evidenced throughout our experiments imply a biosynthetic pathway starting from palmitic acid, in which Δ^6-desaturation or Δ^{11}-desaturation respectively produce the intermediate *E*6-16:Acid and *Z*11-16:Acid gland precursors. Traces of *E*4-14:Acid were found in the gland (Table 3) but no deuterium label incorporation was detected from D_3-14:Acid. In contrast, deuterium labels from D_9-*Z*11-16:Acid were found in both the chain-shortened products *Z*9-14:Acid and the *E*4,*Z*9-14:Acid (Fig. 1E). β-oxidation also takes place from palmitic to myristic acid (Fig. 1C) and likewise the trace *E*4-14:Acid found in the gland is very likely to originate from chain shortening of the corresponding *E*6-16:Acid rather than from a potential Δ^4-desaturation of myristate. Altogether, our results strongly suggested all biosynthetic intermediates to result from Δ^6- and Δ^{11}-desaturation steps.

Candidate fatty acyl-CoA desaturase cDNAs were characterized from the PG tissue using a homology-based PCR approach (*e.g.* Rosenfield et al., 2001; Roelofs et al., 2002; Knipple et al., 2002). Heterologous expression conclusively demonstrated that two desaturases displaying either Δ^6 or Δ^{11} regioselectivity are responsible for the conversion of palmitic acid into the monounsaturated intermediate *E*6- and *Z*11-16:Acid precursors, respectively (Figs. 3 and 4). As demonstrated *in vivo*, the *Z*11-16:Acid can undergo a second Δ6-desaturation to form the immediate *E6,Z*11-16:Acid biosynthetic precursor (Fig. 1B–E). This scenario was confirmed *in vitro* (Figs. 3 and 4) and in addition we showed that an alternative biosynthetic route exists in which the *E6,Z*11-16:Acid is formed through a Δ^{11}-desaturation taking place on the *E*6-16:Acid (Fig. 3D). Eventually, the *E6,Z*11-16:Acid precursor likely undergoes reduction followed by acetylation or oxidation to form its acetate or aldehyde derivatives. It is also chain-shortened to generate the *E4,Z*9-14:Acid prior to subsequent carboxyl end modifications (Fig. 5). Our data support an uncommon pheromone biosynthetic system involving two possible biosynthetic routes to form the immediate pheromone precursor, and depending on the order in which the Δ^6- and Δ^{11}- desaturation reactions take place (Fig. 5). Determining whether a prevalent biosynthetic route may exist *in vivo* (*e.g.* by gene knockdown) may be very difficult to do in this

species since the Δ^6- or Δ^{11}-disrupted enzyme could not produce the intermediate monoenoic substrate necessary for the second enzyme to act upon during the second desaturation step. In spite of this, the large amounts of dienoic precursor produced *in vitro* upon action of the Δ^{11} desaturase may argue in favor of a preferential route involving Δ^6-desaturation of the palmitate to produce the monoenoic *E*6-hexadecenoic acid, followed by Δ^{11}-desaturation to form the *E*6,*Z*11-16:Me (Fig. 5). Alterations in the physical structure of a substrate *(i.e. cis* versus *trans*) have been proposed that could alter the binding efficiency and thus the regio-selectivity and catalytic activity of distinct desaturases (Shanklin et al., 2009). Accordingly, the efficiency of the *Z*11-desaturase (*Ape*-PGΔ11) in forming the dienoic precursor, *i.e.* the *cis* dehydrogenation of a *trans* monounsaturated substrate might be favoured by its easier insertion in the enzyme binding site (Pollard et al., 1980; Shanklin et al., 2009) whereas positional Δ^6 *trans* dehydrogenation might be limited due to the curved structural configuration of the *Z*11-monoene substrate. *Trans* dehydrogenation may overall result in a lower conversion towards the dienoic precursor. Distinct reaction outcomes were also shown for the $\Delta^{12}/\omega3$ positional specificity in a fungal desaturase (Damude et al., 2006) or the sequential $\Delta^{11/11,13}$ desaturation in the moth *Thaumetopoea pityocampa* (Serra et al., 2007).

4.2. Evidence for a pheromone biosynthetic desaturase with Δ^6 regioselectivity in a moth

The formation of Δ^{11}-unsaturated precursors by steaoryl-CoA desaturases in moths is widespread (*e.g.* Knipple et al., 1998; Roelofs et al., 2002; Moto et al., 2004; Serra et al., 2007; Liénard et al., 2008). Moth desaturases typically display a *first*-desaturase activity, *i.e.* they introduce a first double bond in the saturated fatty acyl skeleton (reviewed in Hashimoto et al., 2008). Several examples notably include the cabbage looper moth, *Trichoplusia ni* (Wolf and Roelofs, 1986; Knipple et al., 1998), the corn earworm moth, *Helicoverpa zea* (Rosenfield et al., 2001) and the European corn borer, *Ostrinia nubilalis* (Roelofs et al., 2002). In addition to introducing double bonds in saturated chains, several moth Δ^{11} desaturases further catalyze hydrogen removal from unsaturated fatty-acyls, *e.g.* the *E*11-desaturation that takes places to convert the *E*9-14:acyl into *E*9,*Z*11-14:acyl precursor in the light brown apple moth, *Epiphyas postvittana* (Liu et al., 2002) and the *Z*11-desaturation that takes place on the *Z*9-14:acyl to form the *Z*9,*Z*11-14:acyl precursor in the currant shoot borer, *Lampronia capitella* (Liénard et al., 2008). In *A. pernyi*, both the *Ape*-PGΔ11 and *Ape*-PGΔ6 desaturases exhibit a Δ^{11} activity producing the *Z*11-16:acyl *in vitro*. This suggests that *in vivo*, the *Ape*-PGΔ6 may be the main pheromone production desaturase. However, *Ape*-PGΔ11 also produces a series of Δ^{11}-monoenes including Z11-18:acyl (Fig. 3C), which is in accordance with the gland content and supports the typical moth Δ^{11} desaturase to account for the *in vivo* production of Δ11-acyl intermediates including the *Z*11-16:acyl.

Members of the Δ^{11}-desaturase gene subfamily were characterized that encode enzymes displaying complex bifunctional activities (*e.g.* Moto et al., 2004; Serra et al., 2006, 2007) or unusual regioselectivity such as a recently evidenced Δ^8/Δ^{11}-desaturase gene in *Dendrolimus punctatus* (Lepidoptera: Lasiocampidae) (Liénard et al., 2010). Following this reasoning, one could postulate that an unusual Δ^6 unsaturation in *A. pernyi* may also be introduced by an unusual Δ^{11}-like desaturase. Notwithstanding, our data demonstrate that this Δ^6-desaturase activity results from a distinct enzyme. To date, Δ^6 fatty-acyl desaturases have been characterized from microalgae, plants or animals (Reddy and Thomas, 1996; Sayanova et al., 1997; Napier et al., 1998; Aki et al., 1999; Cho et al., 1999; Hsiao et al., 2007). They belong to a class of desaturases displaying *front-end* activities, which typically introduce an unsaturation between the carboxyl group of a fatty acid and a pre-existing double bond (Sperling et al., 2003; Hashimoto et al., 2008). In particular, Δ^6 desaturases contribute to the biosynthesis of polyunsaturated fatty acids, *e.g.* by converting linoleic acid ($C_{18:2}$, $\Delta^{9,12}$) into γ-linolenic acid ($C_{18:3}$, $\Delta^{6,9,12}$) (Sayanova and Napier, 2004). *Front-end* desaturases share most structural characteristics common to membrane-bound desaturases including several hydrophobic stretches and three conserved histidine regions acting as ligands for the active diiron center, but have a His → Gln substitution in the third his-box and a cytochrome *b5* domain fused to the N-terminus region (Shanklin et al., 1994; Hashimoto et al., 2008). Interestingly, the Δ^6 desaturase in *A. pernyi* exhibits both *first* and *front-end* desaturase activities by producing the *Z*/*E*6-16:Acid and *E*6,*Z*11-16:Acid, respectively. Δ^6 desaturation of linolenic acid has been postulated in the biosynthesis of polyunsaturated hydrocarbon sex pheromones such as in the navel orangeworm, *Amyelois transitella* (Lepidoptera: Pyralidae) (Wang et al., 2010). It would make sense to uncover if this desaturation is catalyzed by an enzyme encoded by an ortholog of the Δ^6 desaturase identified in *A. pernyi*.

4.3. Neofunctionalization in an ancestral desaturase lineage

Different evolutionary scenarios may account for the emergence of the novel Δ^6 moth biosynthetic function and a close examination of desaturase orthologs in other insect lineages is helpful in shedding light on this rare functional occurrence in the Lepidoptera. In the evolution of functionality within desaturase families there exists enzymes exhibiting dual desaturase/hydroxylase or acetylenase/desaturase activity that have retained residual activity of their ancestral gene (Shanklin et al., 2009). This indicates that the Δ^6 enzyme might have conserved a residual Δ^{11} activity if it evolved following a duplication event from an ancestral Δ^{11} desaturase lineage. Alternatively, the ability to display a minor Δ^{11} activity could also have originated independently. Evidence from two extant Δ^{12} desaturases in *Tribolium castaneum* (Coleoptera) and *Acheta domesticus* (Orthoptera) that arose following independent gene duplication events (Fig. 2) (Zhou et al., 2008) likewise supports this scenario. The reconstructed phylogeny reveals the Δ^6 gene to be unrelated to gene members of the Δ^{11} desaturase lineage (Fig. 2), which arose in the early evolution of the Lepidoptera (Liénard et al., 2008). Instead, the new Δ^6 desaturase belongs to a well-supported gene lineage different from biosynthetic Δ^9, Δ^{11} or Δ^{14} desaturases, and that includes orthologs from Lepidoptera (*B. mori*) but also from Diptera (*e.g.*, *Drosophila melanogaster*, *Culex pipiens* and *Aedes aegypti*), Hymenoptera (*Nasonia vitripennis*) and Coleoptera (*Tribolium castaneum*) (Fig. 2). This evidence supports that the gene likely evolved from an ancient duplication event prior to the evolution of Lepidoptera.

A very high degree of synteny is observed between *B. mori* and other lepidopteran genomes (Yasukochi et al., 2009; Beldade et al., 2009) that reflects the comprehensive genome stability across Lepidoptera, making *B. mori* a valuable genomic reference to map gene information from different moth species. In *B. mori*, the closest ortholog of *Ape*-PGΔ11 is the $\Delta^{11/10,12}$ desaturase (Fig. 2), which is located on chromosome 23 (GenBank accession no. BGIBMGA009556), whereas the *B. mori* orthologs of *Ape*-PGΔ6 map onto chromosomes 6 and 21, respectively (GenBank accession nos. BGIBMGA014550 and BGIBMGA01534). *A. pernyi* and *B. mori*, which belong to the same superfamily (Bombycoidea) are reasonably likely to have a similar genome organization; their orthologous desaturase genes should map onto corresponding chromosomes whereas paralogs, which evolved long ago may map to different chromosomes. In addition to the phylogeny, the observed differential chromosomal positioning among *B. mori*

paralogs further supports that both *A. pernyi* Δ^6 and Δ^{11} desaturase paralog genes diverged long ago. Altogether, our data indicate that the most parsimonious evolutionary scenario accounting for the emergence of the novel Δ^6 moth biosynthetic function lies in neo-functionalization from an ancestral insect desaturase lineage, similarly to the evolution of the rare Δ^{14} desaturases of corn borers (Roelofs et al., 2002).

Acknowledgements

The authors are thankful towards Prof. Cai-Hong Wu (Peking University, China) for providing synthetic pheromone standards; Prof. Eric Hedenström and his group (Department of Natural Sciences, Engineering and Mathematics, Sundsvall, Sweden) for synthesizing the *E*6-16:Me, Prof. Zhong-Ning Zhang and Dr. Chao Che (Institute of Zoology, CAS, China) for assistance with chemical synthesis, Dr. Zeng-Liang Chen (Institute of Zoology, CAS, China) for assistance during insect collection and Jean-Marc Lassance (Department of Biology, Lund University, Sweden) for his advice. This study was financially supported by the Swedish research council (Vetenskapsrådet, project no. 621-2007-5659) and VR/SIDA Swedish Research Links (project no. 348-2005-6251), the National Basic Research Program of China (grant no. 2006CB102006) and the National Natural Science Foundation of China (grant no. 30621003).

Appendix. Supplementary data

Supplementary data associated with this article can be found in the online version, at doi:10.1016/j.ibmb.2010.07.009.

References

Aki, T., Shimada, Y., Inagaki, K., Higashimoto, H., Kawamoto, S., Shigeta, S., Ono, K., Suzuki, O., 1999. Molecular cloning and functional characterization of rat delta-6 fatty acid desaturase. Biochem. Biophys. Res. Commun. 255, 575–579.

Ando, T., Inomata, S., Yamamoto, M., 2004. Lepidopteran sex pheromones. Topics Curr. Chem. 239, 951–961.

Attygalle, A.B., 1998. Microchemical techniques. In: Millar, J.G., Haynes, K.F. (Eds.), Methods in Chemical Ecology. Chemical Methods, vol. I. Springer, New York, pp. 229–238.

Beldade, P., Saenko, S., Pul, N., Long, A., 2009. A gene-based linkage map for *Bicyclus anynana* butterflies allows for a comprehensive analysis of synteny with the lepidopteran reference genome. PLoS Genet. 5, e10000366. doi:10.1371/journal.pgen.1000366.

Bestmann, H.J., Attygalle, A.B., Brosche, T., Erler, J., Platz, H., Schwarz, J., Vostrowsky, O., Wu, C.H., Kaissling, K.E., Chen, T.M., 1987. Identification of three sex pheromone components of the female Saturniid moth *Antheraea pernyi* (Lepidoptera: Saturniidae). Z. Naturforsch. 42c, 631–636.

Bjostad, L.B., Wolf, W., Roelofs, W.L., 1987. Pheromone biosynthesis in lepidopterans: desaturation and chain shortening. In: Blomquist, G.J., Prestwich, G.D. (Eds.), Pheromone Biochemistry. Academic Press, New-York, pp. 77–120.

Blomquist, G.J., Jurenka, R.A., Schal, C., Tittiger, C., 2005. Biochemistry and molecular biology of pheromone production. In: Gilbert, L.I., Iatrou, K., Gill, S. (Eds.), Comprehensive Molecular Insect Science. Elsevier Academic, Oxford, pp. 705–752.

Buser, H.-R., Arn, H., Guerin, P., Rauscher, S., 1983. Determination of double bond position in mono-unsaturated acetates by mass spectrometry of dimethyl disulfide adducts. Anal. Chem. 55, 818–822.

Cho, H., Nakamura, M., Clarke, S., 1999. Cloning, expression, and nutritional regulation of the mammalian delta-6 desaturase. J. Biol. Chem. 274, 471–477.

Damude, H., Zhang, H., Farrall, L., Ripp, K., Tomb, J., Hollerbach, D., Yadav, N., 2006. Identification of bifunctional Δ12/ω3 fatty acid desaturases for improving the ratio of ω3 to ω6 fatty acids in microbes and plants. Proc. Natl. Acad. Sci. U.S.A. 103, 9446–9451.

Dunkelblum, S.H., Silk, P.J., 1985. Double bond location in monounsaturated fatty acids by dimethyl disulfide derivatization and mass spectrometry: application to analysis of fatty acids in pheromone glands of four lepidoptera. J. Chem. Ecol. 11, 265–277.

Hashimoto, K., Yoshizawa, A., Okuda, S., Kuma, K., Goto, S., Kanehisa, M., 2008. The repertoire of desaturases and elongases reveals fatty acid variations in 56 eukaryotic genomes. J. Lip. Res. 49, 183–191.

Hsiao, T.Y., Holmes, B., Blanch, H.W., 2007. Identification and functional analysis of a delta6 desaturase from the marine microalga *Glossomastix chrysoplasta*. Mar. Biotechnol. 9, 154–165.

Katoh, K., Toh, H., 2008. Recent developments in the MAFFT multiple sequence alignment program. Brief. Bioinform. 9, 286–298.

Knipple, D.C., Rosenfield, C.-L., Miller, S.J., Liu, W., Tang, J., Ma, P.W.K., Roelofs, W.L., 1998. Cloning and functional expression of a cDNA encoding a pheromone gland-specific acyl-CoA Delta11- desaturase of the cabbage looper moth, *Trichoplusia ni*. Proc. Natl. Acad. Sci. U.S.A. 95, 15287–15292.

Knipple, D.C., Rosenfield, C.-L., Nielsen, R., You, K.M., Jeong, S.E., 2002. Evolution of the integral membrane desaturase gene family in moths and flies. Genetics 162, 1737–1752.

Kochansky, J., Tette, J., Taschenberg, E.F., Cardé, R.T., Kaissling, K.-E., Roelofs, W.L., 1975. Sex pheromone of the moth *Antheraea polyphemus*. J. Insect Physiol. 21, 1977–1983.

Liénard, M.A., Strandh, M., Hedenström, E., Johansson, T., Löfstedt, C., 2008. Key biosynthetic gene subfamily recruited for pheromone production prior to the extensive radiation of Lepidoptera. BMC Evol. Biol. 8, 270.

Liénard, M.A., Lassance, J.-M., Wang, H.-L., Zhao, C.-H., Piškur, J., Johansson, T., Löfstedt, C., 2010. Elucidation of the sex-pheromone biosynthesis producing 5,7-dodecadienes in *Dendrolimus punctatus* (Lepidoptera: Lasiocampidae) reveals Δ11- and Δ9-desaturases with unusual catalytic properties. Insect Biochem. Mol. Biol. 40, 440–452.

Liu, W., Jiao, H., O'Connor, M., Roelofs, W.L., 2002. Moth desaturase characterized that produces both *Z* and *E* isomers of delta11-tetradecenoic acids. Insect Biochem. Mol. Biol. 32, 1489–1495.

Liu, W., Rooney, A.P., Xue, B., Roelofs, W.L., 2004. Desaturases from the spotted fireworm moth (*Choristoneura parallela*) shed light on the evolutionary origins of novel moth sex pheromone desaturases. Gene 342, 303–311.

Löfstedt, C., Hansson, B.S., Tóth, M., Szöcs, G., Buda, V., Bengtsson, M., Ryrholm, N., Svensson, M., Priesner, E., 1994. Pheromone differences between sibling taxa *Diachrysia chrysitis* (Linnaeus, 1758) and *D. tutti* (Kostrowicki, 1961) (Lepidoptera: Noctuidae). J. Chem. Ecol. 20, 91–109.

Moto, K., Suzuki, M.G., Hull, J.J., Kurata, R., Takahashi, S., Yamamoto, M., Kazuhiro, O., Imai, K., Ando, T., Matsumoto, S., 2004. Involvement of a bifunctional fatty-acyl desaturase in the biosynthesis of the silkmoth, *Bombyx mori*, sex pheromone. Proc. Natl. Acad. Sci. U.S.A. 101, 8631–8636.

Naka, H., Vang, L.V., Inomata, S.-I., Ando, T., Kimura, T., Honda, H., Tsuchida, K., Sakurai, H., 2003. Sex pheromone of the persimmon fruit moth, *Stathmopoda masinissa*: identification and laboratory bioassay of (4 *E*,6 *Z*)-4,6-hexadecadien-1-ol derivatives. J. Chem. Ecol. 29, 2447–2459.

Napier, J.A., Hey, S., Lacey, D., Shewry, P., 1998. Identification of a *Caenorhabditis elegans* delta-6 fatty-acid desaturase by heterologous expression in *Saccharomyces cerevisiae*. Biochem. J. 330, 611–614.

Patel, O., Fernley, R., Macreadie, I., 2003. *Saccharomyces cerevisiae* expression vectors with thrombin-cleavable N- and C-terminal 6x(His) tags. Biotechnol. Lett. 25, 331–334.

Percy-Cunningham, J.E., MacDonald, J.A., 1987. Biology and ultrastructure of sex pheromone producing glands. In: Blomquist, G.J., Prestwich, G.D. (Eds.), Pheromone Biochemistry. Academic Press, New York, pp. 27–76.

Pollard, M.R., Gunstone, F.D., James, A.T., Morris, L.J., 1980. Desaturation of positional and geometric isomers of monoenoic fatty acids by microsomal preparations from rat liver. Lipids 15, 306–314.

Reddy, A.S., Thomas, T.L., 1996. Expression of a cyanobacterial Δ^6-desaturase gene results in γ-linolenic acid production in transgenic plants. Nat. Biotechnol. 14, 639–642.

Roelofs, W.L., Bjostad, L., 1984. Biosynthesis of Lepidopteran pheromones. Bioorg. Chem. 12, 279–298.

Roelofs, W.L., 1995. Chemistry of sex attraction. Proc. Natl. Acad. Sci. U.S.A. 92, 44–49.

Roelofs, W.L., Liu, W., Hao, G., Jiao, H., Rooney, A.P., Linn Jr., C.E., 2002. Evolution of moth sex pheromones via ancestral genes. Proc. Natl. Acad. Sci. U.S.A. 99, 13621–13626.

Roelofs, W.L., Rooney, A.P., 2003. Molecular genetics and evolution of pheromone biosynthesis in Lepidoptera. Proc. Natl. Acad. Sci. U.S.A. 100, 9179–9184.

Rosenfield, C.-L., You, K.M., Herrick-Marsella, P., Roelofs, W.L., Knipple, D.C., 2001. Structural and functional conservation and divergence among acyl-CoA desaturases of two noctuid species, the corn earworm, *Helicoverpa zea*, and the cabbage looper, *Trichoplusia ni*. Insect Biochem. Mol. Biol. 31, 949–964.

Sayanova, O.V., Smith, M.A., Lapinskas, P., Stobart, A.K., Dobson, G., Christie, W.W., Shewry, P.R., Napier, J.A., 1997. Expression of a borage desaturase cDNA containing an N-terminal cytochrome b_5 domain results in the accumulation of high levels of Δ^6-desaturated fatty acids in transgenic tobacco. Proc. Natl. Acad. Sci. U.S.A. 94, 4211–4216.

Sayanova, O.V., Napier, J.A., 2004. Eicosapentaenoic acid: biosynthetic routes and the potential for synthesis in transgenic plants. Phytochemistry 65, 147–158.

Schneiter, R., Tatzer, V., Gogg, G., Leitner, E., Kohlwein, S.D., 2000. Elo1-dependent carboxy-terminal elongation of C14:1Delta(9) to C16:1Delta(11) fatty acids in *Saccharomyces cerevisiae*. J. Bacteriol. 182, 3655–3660.

Serra, M., Piña, B., Bujons, J., Camps, F., Fabriàs, G., 2006. Biosynthesis of 10,12-dienoic fatty acids by a bifunctional Ä11 desaturase in *Spodoptera littoralis*. Insect Biochem. Mol. Biol. 36, 634–641.

Serra, M., Piña, B., Abad, J.L., Camps, F., Fabriàs, G., 2007. A multifunctional desaturase involved in the biosynthesis of the processionary moth sex pheromone. Proc. Natl. Acad. Sci. U.S.A. 104, 16444–16449.

Shanklin, J., Whittle, E., Fox, B.G., 1994. Eight histidine residues are catalytically essential in a membrane-associated iron enzyme, stearoyl-CoA desaturase, and

are conserved in alkane hydroxylase and xylene monooxygenase. Biochemistry 33, 12787–12794.
Shanklin, J., Cahoon, E.B., 1998. Desaturation and related modifications of fatty acids. Annu. Rev. Plant Physiol. Plant Mol. Biol. 49, 611–641.
Shanklin, J., Guy, J.E., Mishra, G., Lindqvist, Y., 2009. Desaturases: emerging models for understanding functional diversification of Diiron-containing enzymes. J. Biol. Chem. 284, 18559–18563.
Sperling, P., Ternes, P., Zank, T.K., Heinz, E., 2003. The evolution of desaturases. Prostag. Leukotr. Ess. 68, 73–95.
Tamura, K., Nei, M., Kumar, S., 2007. MEGA4: Molecular evolutionary genetics analysis software version 4.0. Mol. Biol. Evol. 24, 1596–1599.
Tillman, J.A., Seybold, S.J., Jurenka, R.A., Blomquist, G.J., 1999. Insect pheromones-an overview of biosynthesis and endocrine regulation. Insect Biochem. Mol. Biol. 29, 481–514.
Wang, H.L., Zhao, C.H., Millar, J.G., Cardé, R.T., Löfstedt, C., 2010. Biosynthesis of unusual moth pheromone components involves two different pathways in the navel orangeworm, *Amyelois transitella*. J. Chem. Ecol. 36, 535–547.
Wolf, W.A., Roelofs, W.L., 1986. Properties of the Δ11-desaturase enzyme used in cabbage looper moth sex pheromone biosynthesis. Arch. Insect Biochem. Physiol. 3, 45–52.
Yasukochi, Y., Tanaka-Okuyama, M., Shibata, F., Yoshido, A., Marec, F., Wu, C., Zhang, H., Goldsmith, M., Sahara, K., 2009. Extensive conserved synteny of genes between the karyotypes of *Manduca sexta* and *Bombyx mori* revealed by BAC-FISH mapping. PloS One 4, e7465. doi:10.1371/journal.pone.0007465.
Zhou, X.-R., Horne, I., Damcevski, K., Haritos, V., Green, A., Singh, S., 2008. Isolation and functional characterization of two independently-evolved fatty acid Ä12-desaturase genes from insects. Insect Mol. Biol. 17, 667–676.